Direct measurement of quantum Fisher information

Xingyu Zhang [1], Xiao-Ming Lu [2], Jing Liu [3], Wenkui Ding [4] and Xiaoguang Wang [5,*]

[1] *Zhejiang Institute of Modern Physics, Department of Physics, Zhejiang University, Hangzhou 310027, China*

[2] *School of Sciences, Hangzhou Dianzi University, Hangzhou 310018, China*

[3] *MOE Key Laboratory of Fundamental Physical Quantities Measurement, National Precise Gravity Measurement Facility, School of Physics, Huazhong University of Science and Technology, Wuhan 430074, China*

[4] *Beijing National Laboratory for Condensed Matter Physics, Institute of Physics, Chinese Academy of Sciences, Beijing 100190, China*

[5] *Key Laboratory of Optical Field Manipulation of Zhejiang Province and Department of Physics, Zhejiang Sci-Tech University, Hangzhou 310018, China*

(Received 7 August 2022; revised 2 November 2022; accepted 13 December 2022; published 10 January 2023)

In the adiabatic perturbation theory, Berry curvature is related to the generalized force, and the quantum metric tensor is linked with energy fluctuation. While the former is tested with numerous numerical results and experimental realizations, the latter is less considered. Quantum Fisher information, the key to quantum precision measurement, is a four times quantum metric tensor. It is difficult to relate the quantum Fisher information with some physical observable. One interesting candidate is the square of the symmetric logarithmic derivative, which is usually tough to obtain, both theoretically and experimentally. The adiabatic perturbation theory enlightens us to measure the energy fluctuation to directly extract the quantum Fisher information. In this article we first adopt an alternative way to derive the link of energy fluctuation to the quantum Fisher information. Then we numerically testify to the direct extraction of the quantum Fisher information based on adiabatic perturbation in two-level systems and simulate the experimental realization in a nitrogen-vacancy center with experimentally practical parameters. Statistical models such as the transverse-field Ising model and Heisenberg spin chains are also discussed to compare with the analytical result and show the level crossing, respectively. Our discussion will provide a practical scheme to measure the quantum Fisher information and will also be a benefit to quantum precision measurement and the understanding of the quantum Fisher information.

DOI: 10.1103/PhysRevA.107.012414

I. INTRODUCTION

Quantum Fisher information (QFI) and the quantum Fisher information matrix (QFIM) are at the heart of quantum precision measurement theory [1–6]. The QFI is usually denoted by F_λ and, originating from the classical Fisher information, depicts how much information a quantum state contains for the metrology of a certain parameter. In the usual unbiased estimation process, the estimator for the parameter λ, constructed from other experimental parameter outcomes, is assumed to have an expectation equal to the real value of the parameter λ. And the sensitivity of the parameter, described by the variance of the estimator $\Delta^2\lambda$, is lower bounded by the reciprocal of QFI, $1/F_\lambda$, known as the quantum Cramér-Rao bound. As a result, larger quantum Fisher information is required for better estimation of the corresponding parameter. QFIM $F_{\mu\nu}$ is a generalization of QFI and is crucial to the multiparameter estimation. Although the QFI is crucial in the measurement theory, recently a few schemes [7–13] were proposed for the direct extraction of the QFI. Moreover, the calculation of the QFI is not that simple, and the expression of the estimating state is even not known. This remains an interesting problem in the quantum measurement. Inspired by the work of Ref. [14], we notice that the adiabatic perturbation may be a starting point for the measurement of QFI, and a physical quantity naturally emerges from that.

The quantum geometric tensor [15–18] consists of two important physical quantities, i.e., the Berry curvature corresponding to its imaginary part, and the quantum metric tensor corresponding to its real part. The former is an intrinsic topological quantity, and its integral gives the Chern number [19,20]. The latter is usually less considered in condensed-matter theory, but it plays a better role in quantum precision measurement since it is exactly a quarter of QFIM. Since the Berry curvature is particularly important in topological physics, it is useful to find a way to measure it directly [21–24]. It has been realized that the Berry curvature emerges as the dynamical response in the nonadiabatic evolution. An excellent tool is the adiabatic perturbation theory [25–32], which regards the quantum adiabatic approximation as the zeroth-order case and depicts a perturbation extension in terms of the small parameter's changing rate v to correct the quantum adiabatic theorem. In the work of Gritsev and Polkovnikov [14], they used the result from adiabatic perturbation theory to calculate the linear response of a slowly driven system, and the Berry curvature emerges due to the quench. This means

$$-\langle\psi(t_f)|\partial_\mu H|\psi(t_f)\rangle = \text{const} + \mathcal{B}_{\mu\lambda}v_\lambda + O(v^2), \quad (1)$$

where the quench velocity $v_\lambda = \dot{\lambda}$ is the changing rate of the parameter, and the above quantities are evaluated in the final time t_f. The decorated $\mathcal{B}_{\mu\nu}$ is the Berry curvature of the

*xgwang1208@zju.edu.cn

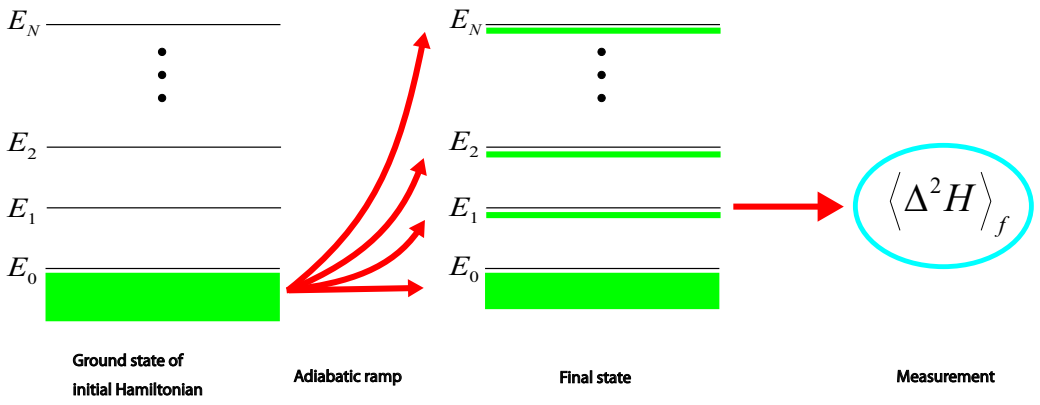

FIG. 1. Illustration of the extraction of the QFI (matrix). The initial state is prepared to be the ground state of the initial Hamiltonian. (The green block represents the population in each level and it is located in the ground state, obviously.) Then the parameter(s) of the Hamiltonian is (are) slowly changed with vanishing switching-on velocity. The populations in higher levels are still small but not zero due to quasiadiabaticity. When the Hamiltonian is evolved into the interested one, the energy fluctuation is measured in the final state of the system. The ratio between the expectation to the square of the final velocity of parameter(s) gives the QFI (matrix).

ground state of the final Hamiltonian. The left-hand side of the equation is called the generalized force. This remarkable finding can benefit the direct measurement of the Berry curvature and even the topological transition [33–36], regardless of the system's size and interaction strength. On the other hand, in the work [31,37] they achieve a similar result concerning the quantum metric tensor; hence we find a way to directly measure the QFIM in the context of adiabatic perturbation. The results can be written as the following expressions with respect to QFIM:

$$\langle \psi(t_f)|\Delta^2 H|\psi(t_f)\rangle = \frac{1}{4}F_\lambda {v_\lambda}^2 + O(v^3), \tag{2}$$

$$\langle \psi(t_f)|\Delta^2 H|\psi(t_f)\rangle = \frac{1}{4}\sum_{\mu\nu} F_{\mu\nu} v^2 + O(v^3). \tag{3}$$

F_λ and $F_{\mu\nu}$ are the QFI and QFIM, respectively, of the ground state of the final time Hamiltonian. The ground state of a Hamiltonian is extremely important, since it exhibits the properties of the system, e.g., quantum phase transition [38]. When two parameters are slowly driven with the same time-dependent part, the result gives the sum of QFIM entities (3). These results show that the QFI of the ground state of the corresponding final Hamiltonian can be directly observed as the slope of the expectation value of energy fluctuation with respect to the square of the parameter's changing velocity. Therefore we can measure the QFI of the ground state of nondegenerate Hamiltonians even if the ground state is not expressed explicitly. In contrast with Eq. (1), Eqs. (2) and (3) are often not considered and not verified with numerical and experimental simulation. In this article, we depict how to use these results to extract the QFI and QFIM. Furthermore, the experimental setup is considered with the nitrogen-vacancy center. The illustration of whole QFI (matrix) extraction protocol is Fig. 1.

This paper is divided into four parts. We first describe how to obtain Eqs. (2) and (3) using a different way from that of Refs. [31,37]. Then we use a two-level system to demonstrate the validity of our method. Next, we briefly discuss the experimental protocols via the NV center. Third, we exhibit the applications of our result to the statistical models, i.e., a one-dimensional transverse-field Ising model and Heisenberg spin chains, to testify as to their validity and utility. Since the one-dimensional transverse-field Ising model can be solved analytically, this provides a wonderful platform for us to compare our method with the analytic result. It is shown that our method matches the result of the standard procedure of diagonalization well. The last part concludes our work and gives some discussion.

II. MEASURING THE QFI OF THE GROUND STATE USING ADIABATIC PERTURBATION

In this part we will provide a method to measure the QFI and QFIM of certain ground states based on the adiabatic perturbation. It is known that for a Hamiltonian $H(\lambda(t))$, the spectrum can be expressed as

$$H(\lambda(t))|\phi_n(\lambda(t))\rangle = E_n(\lambda(t))|\phi_n(\lambda(t))\rangle, \tag{4}$$

where $|\phi_n\rangle$ is the nth eigenstate of the Hamiltonian H with the eigenvalue E_n. We assume that the spectrum is finite and the Hamiltonian is nondegenerate. The QFI of the ground state $|\phi_0\rangle$ of the Hamiltonian is

$$\begin{aligned} F_\lambda &= 4(\langle \partial_\lambda \phi_0|\partial_\lambda \phi_0\rangle - \langle \partial_\lambda \phi_0|\phi_0\rangle\langle \phi_0|\partial_\lambda \phi_0\rangle) \\ &= 4\sum_{n\neq 0}\langle \partial_\lambda \phi_0|\phi_n\rangle\langle \phi_n|\partial_\lambda \phi_0\rangle \\ &= 4\sum_{n\neq 0}|\langle \partial_\lambda \phi_0|\phi_n\rangle|^2. \end{aligned} \tag{5}$$

To directly measure the QFI, we need to connect it with some observables.

In contrast with the method of [31,37], we give an alternative approach to prove Eqs. (2) and (3). First, we follow the work of Berry and Robbins [39] to do the adiabatic expansion. By using a small constant ϵ, called the adiabatic parameter, to change the timescale as $t \to t/\epsilon$, the Schrödinger equation becomes

$$i\epsilon\frac{d\rho(t)}{dt} = [H(\lambda(t)), \rho(t)], \tag{6}$$

where the time-dependent quantities are rewritten with the new timescale, i.e., $\rho(t/\epsilon) \to \rho(t)$ and $\lambda(t/\epsilon) \to \lambda(t)$.

Berry and Robbins [39] expanded the density operator of the evolving state as

$$\rho(t) = \sum_{r=0}^{\infty} \epsilon^r \rho_r(t), \tag{7}$$

where the rth order $\rho_r(t)$ is required to satisfy

$$[H, \rho_0] = 0, \tag{8}$$

$$[H, \rho_r] = i\dot{\rho}_{r-1} \quad \forall\, r > 0. \tag{9}$$

It is easy to verify from Eqs. (8) and (9) that $\rho(t)$ given by Eq. (7) satisfies the Schrödinger equation. Let $|\phi_k\rangle$ be the instantaneous eigenstate of H with the instantaneous eigenvalue E_k. It follows from Eq. (9) that the off-diagonal elements of ρ_r can be determined by the time derivative of ρ_{r-1} as [39]

$$\langle\phi_k|\rho_r|\phi_l\rangle = i\frac{\langle\phi_k|\dot{\rho}_{r-1}|\phi_l\rangle}{E_k - E_l} = i\dot{\lambda}\frac{\langle\phi_k|\partial_\lambda\rho_{r-1}|\phi_l\rangle}{E_k - E_l} \tag{10}$$

for all $k \neq l$. The diagonal elements of ρ_r should be determined by other conditions in addition to Eqs. (8) and (9), as the sum of ρ_r and any other constant operator that is simultaneously diagonalizable with H still satisfies Eq. (9).

Assume that the system is initially in the ground state of the Hamiltonian. In such a case, ρ_0 is chosen as the adiabatic state $|\phi_0\rangle\langle\phi_0|$, i.e., the instantaneous ground state at time t, which obviously satisfies the condition given by Eq. (8). We shall investigate the adiabatic expansion of the expectation $\mathrm{Tr}[(H - E_0)^2\rho]$:

$$\mathrm{Tr}[(H - E_0)^2\rho] = \sum_{r=0}^{\infty} \epsilon^r \,\mathrm{Tr}[(H - E_0)^2\rho_r]. \tag{11}$$

We can use the basis constituted by the instantaneous eigenstates of H to represent the operators, that is,

$$\mathrm{Tr}[(H - E_0)^2\rho] = \sum_{k>0}(E_k - E_0)^2 p_k, \tag{12}$$

where p_k for $k > 0$ is the transition probability defined as

$$p_k := \langle\phi_k|\rho|\phi_k\rangle = \sum_{r=1}^{\infty} \epsilon^r \langle\phi_k|\rho_r|\phi_k\rangle. \tag{13}$$

Berry and Robbins [39] used the pure state condition, $\rho(t) = \rho(t)^2$, to determine the diagonal elements of ρ_r. Using the adiabatic expansion $\rho = \sum_r \epsilon^r \rho_r$, the pure state condition can be written as

$$\sum_{r=0}^{\infty} \epsilon^r \rho_r = \sum_{r=0}^{\infty}\sum_{s=0}^{\infty} \epsilon^{r+s} \rho_r \rho_s. \tag{14}$$

The zeroth approximation of the above equality automatically holds, as the adiabatic state ρ_0 is a pure state. It then follows from the first-order approximation $\rho_1 = \rho_0\rho_1 + \rho_1\rho_0$ that

$$\langle\phi_k|\rho_1|\phi_k\rangle = 2\delta_{0k}\langle\phi_k|\rho_1|\phi_k\rangle, \tag{15}$$

meaning that $\langle\phi_k|\rho_1|\phi_k\rangle = 0$. To the second-order approximation, the pure state condition implies that $\rho_2 = \rho_0\rho_2 + \rho_1\rho_1 + \rho_2\rho_0$. For $k \neq 0$ it follows that

$$\langle\phi_k|\rho_2|\phi_k\rangle = \sum_l \langle\phi_k|\rho_1|\phi_l\rangle\langle\phi_l|\rho_1|\phi_k\rangle. \tag{16}$$

Combining the condition Eq. (9) and the first-order approximation of the pure state condition, it can be shown that

$$\langle\phi_k|\rho_1|\phi_l\rangle = \begin{cases} i\dot{\lambda}\frac{\langle\phi_k|\partial_\lambda\phi_l\rangle(\delta_{0l} - \delta_{0k})}{E_k - E_l}, & \text{if } k \neq l, \\ 0, & \text{if } k = l. \end{cases} \tag{17}$$

Substituting Eqs. (16) and (17) into Eq. (12) and neglecting the higher-order terms, we get

$$\begin{aligned}\mathrm{Tr}[(H - E_0)^2\rho] &\approx \epsilon^2 \sum_{k\neq 0}\langle\phi_k|\rho_2(t)|\phi_k\rangle(E_k - E_0)^2 \\ &= \epsilon^2\dot{\lambda}^2 \sum_{k\neq 0} |\langle\phi_k|\partial_\lambda\phi_0\rangle|^2.\end{aligned} \tag{18}$$

Note that the adiabatic parameter ϵ can be absorbed into the velocity of λ as $\epsilon\dot{\lambda} \to \dot{\lambda}$ when we change to the original timescale. We denote the quantity $(H - E_0)^2$ as the square of the absolute Hamiltonian (SAH), since the eigenvalues of this quantity are independent of the choice of the zero of the energy. Since SAH is different from the energy fluctuation by high-order negligible quantities, i.e.,

$$\begin{aligned}&\langle(H - E_0)^2\rangle - \langle(H - \langle H\rangle)^2\rangle \\ &\quad = (\langle H\rangle - E_0)^2 \\ &\quad = \left(\sum_{n\neq 0} |a_n(\lambda_f)|^2 E_n\right)^2 \sim O(\dot{\lambda}^4),\end{aligned} \tag{19}$$

we then recover the result Eq. (2), as briefly discussed in [31,37]. From this expression, once we obtain the expectation of the $\Delta^2 H$ or $(H - E_0)^2$ at the final time, the QFI of the ground state of the final Hamiltonian H can be seen from the proportional coefficient with respect to the square of velocity $\dot{\lambda}_f^2$. The subscript f denotes quantity at the final time.

We can conclude the measurement procedure above as follows. We set the estimating parameter of the Hamiltonian at arbitrary initial value and the initial state at the ground state. Then we evolve the parameter of the Hamiltonian to the required value, and the evolving velocity needs to be very slow. At the final time, we measure the energy fluctuation or SAH in the instantaneous state. The ratio of expectation with respect to the square of final time parameter's changing velocity gives a quarter of QFI of the ground state of the final time Hamiltonian. We do not need to calculate the explicit expression of the final time ground state.

We now move to the extraction of the multiparameter QFIM. Inspired by the work of Ozawa and Goldman [7], we use a two-parameter modulation to extract the multiparameter QFIM. When the arbitrarily selected two parameters share the same time-dependent part, i.e., $\lambda_1 = C + f(t)$ and $\lambda_2 = D + f(t)$, Eq. (17) becomes

$$\langle\phi_k|\rho_1(t)|\phi_l\rangle = i\dot{\lambda}\frac{\sum_\mu\langle\phi_k|\partial_\mu\phi_l\rangle(\delta_{0l} - \delta_{0k})}{E_k - E_l}, \ (k \neq l), \tag{20}$$

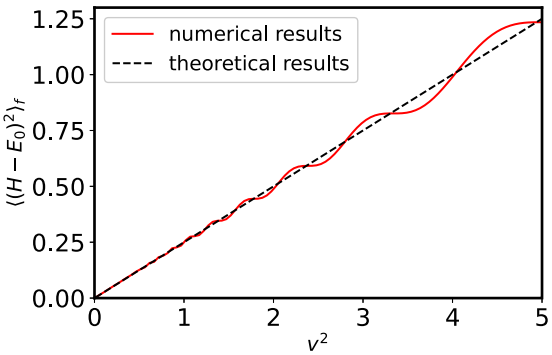

FIG. 2. Measurement of the QFI with respect to θ, F_θ, of the ground state of a two-level system. The numerical result is obtained by the dynamical simulation using the software packages developed in Refs. [40,41].

and Eq. (18) is corrected as

$$\mathrm{Tr}[(H-E_0)^2\rho(t)] = \epsilon^2\dot{\lambda}^2 \sum_{\mu\nu=1}^{2} \sum_{k\neq 0} \langle \partial_\mu \phi_0 | \phi_k \rangle \langle \phi_k | \partial_\nu \phi_0 \rangle, \quad (21)$$

where $\dot{\lambda} = df(t)/dt$ is the velocity of both parameters. The ratio between the final expectation of the SAH and the parameters' velocity gives a quarter of the sum of QFIM elements, as in Eq. (3). Notably, C and D are time-independent constants, and their difference should be set to satisfy the difference between our anticipated final λ_1, λ_2. The time-dependent part $f(t)$ is not necessarily periodically small perturbation and constrained only by the adiabatic conditions. Since $F_{\lambda_1\lambda_1}$ and $F_{\lambda_2\lambda_2}$ can be extracted from Eq. (18), the off-diagonal multiparameter QFI $F_{\lambda_1\lambda_2}$ is easily obtained. Next we show the feasibility of the measurement protocol on QFI and QFIM in the context of adiabatic perturbation.

These results can be testified within a two-level system. We consider the following typical Hamiltonian,

$$H(t) = B\boldsymbol{n}(t)\cdot\boldsymbol{\sigma}, \quad (22)$$

where $\boldsymbol{n}(t)$ is a three-component vector defined as $\boldsymbol{n}(t) = (\sin\theta\cos\phi, \sin\theta\sin\phi, \cos\theta)$. In this situation, we follow the proposal of Ref. [14] and set the polar angle $\theta = \frac{v^2t^2}{2\pi}$ and the azimuthal angle $\phi = 0$. This kind of ramp can make the initial parameter's velocity vanish to lift the oscillation caused by the initial state; otherwise an extra integration process is required, as discussed in Ref. [33]. Actually, any ramp satisfying $\dot{\lambda}(t)|_{t=0} = 0$ and $\dot{\lambda}(t)|_{t=t_f} = v$ is the candidate, where t_f is the final time, v is the final velocity, and we want to incorporate v into the function $\lambda(t)$ to serve as a constant denoting the evolving velocity. The ground state of the initial Hamiltonian is $(0, 1)^T$, and it evolves with the time-dependent Hamiltonian until the final time $t_f = \frac{\pi}{v}$. At the final state, the observable $(H-E_0)^2$ or $\Delta^2 H$ is measured. Since the parameter's changing velocity at last is just v, the QFI of the ground state of the final Hamiltonian H is obtained. The theoretical computation of the final QFI is unity, and the above procedure gives the same result from the Fig. 2.

In order to validate Eq. (21), we construct a nontrivial two-level example since the Hamiltonian (22) with θ and ϕ as parameters has vanishing off-diagonal quantum Fisher information. We still use the form Eq. (22), but the vector becomes $\boldsymbol{n}(t) = [\sin(x+y)\cos(xy), \sin(x+y)\sin(xy), \cos(x+y)]$, where x and y are the parameters to be estimated. The parameters are driven as follows: $x(t) = x(0) + \frac{v^2t^2}{2\pi}$ and $y(t) = \frac{v^2t^2}{2\pi}$. The final time $t_f = \frac{\pi}{v}$ parameters' changing velocities are both v. Using our method, we plot the function of the sum of Fisher information matrix elements with respect to the initial $x(0)$. The QFIM is evaluated at the final time Hamiltonian's ground state with respect to $x(t_f) = x(0) + \frac{\pi}{2}$ and $y(t_f) = \frac{\pi}{2}$. From Fig. 3 we find that our method matches the exact solution perfectly.

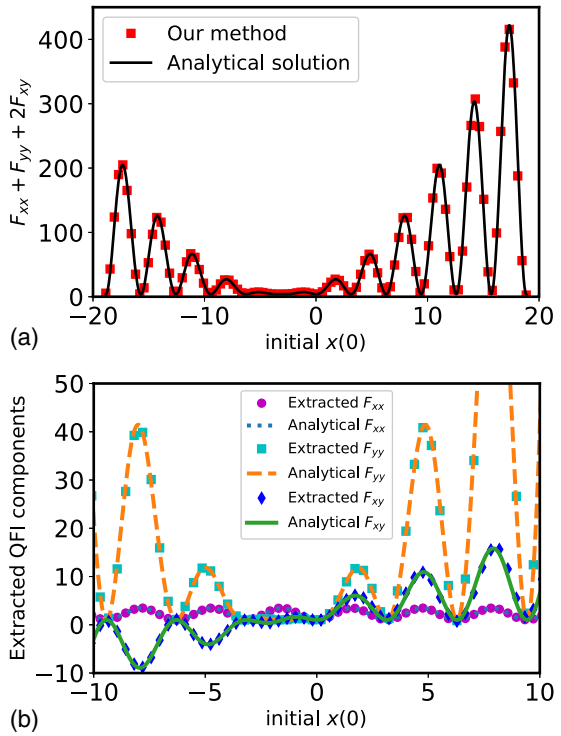

FIG. 3. (a) Sum of elements of the QFIM with respect to $x(0)$ when the final Hamiltonian's ground state is estimated. (b) Diagonal elements of the QFIM evaluated using Eq. (18) and off-diagonal elements of the QFIM obtained using half of the difference between the sum of all QFIM elements and all the diagonal QFIM elements.

III. EXPERIMENTAL CONSIDERATION

We now carry out some experimental discussions. Here we choose the nitrogen-vacancy (NV) center [42–46] in diamond as the applicable settings and employ the work of Yu *et al.* to exhibit our measuring procedure. The NV center has three sublevels $m_s = 0, \pm 1$, and by using external magnetic field $B_z \simeq 510$ Gauss can lift the degeneracy between $|+1\rangle$ and $|-1\rangle$. Then the two lower sublevels $|0\rangle$ and $|-1\rangle$ constitute a two-level system with a gap $\omega_0 = D - \gamma_e B_z$, where the $D = 2\pi \times 2.87$ GHz is the zero-field splitting and γ_e is the electronic gyromagnetic ratio, as is depicted in Fig. 4(a). We need to prepare the system in the ground state of the interested Hamiltonian. The initialization procedure includes the 532-nm green laser, which put the NV center in the $m_s = 0$ state. Using an arbitrary wave-form generator can drive the

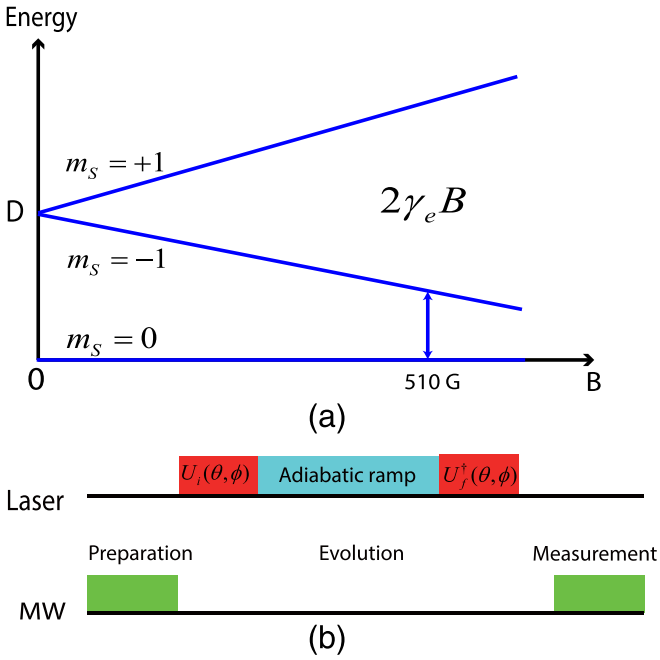

FIG. 4. (a) Energy splitting first due to the zero-field splitting D and then the external field B. (b) Demonstration of the protocol of measuring QFI in NV center.

transition between levels $|0\rangle$ and $|-1\rangle$, and the Hamiltonian of the laboratory frame is [9,47,48]

$$H = \frac{\omega_0}{2}\sigma_z + V(t)\sigma_x, \tag{23}$$

where $V(t) = A\sin\theta(t)\cos[\omega_0 t - \Theta(t) + \phi]$, A is the amplitude incorporating an electron gyromagnetic ratio into itself, and θ (or ϕ) is the estimated parameter. Here the phase control function is set as $\Theta(t) = A\int_0^t \cos\theta(\tau)d\tau$. Under a rotation operator $e^{iR(t)} = e^{i\frac{1}{2}(\omega_0 t - \Theta(t))\sigma_z}$, the effective Hamiltonian in the rotating frame can take the form of [9,47]

$$\begin{aligned} H_{\text{eff}} &= e^{iR(t)}He^{-iR(t)} + i\frac{\partial e^{iR(t)}}{\partial t}e^{-iR(t)} \\ &\simeq \frac{A}{2}(\sin\theta\cos\phi\sigma_x + \sin\theta\sin\phi\sigma_y + \cos\theta\sigma_z), \end{aligned} \tag{24}$$

where we used the rotating wave approximation. The relations between energy fluctuation in the original frame and that in the rotating frame are illustrated in Appendix.

We list the whole procedures as follows, and Fig. 4(b) shows these operations diagrammatically.

(1) *Preparation of initial states.* Applying a microwave field can take the initial state from the $m_s = 0$ state to the ground state of the initial H_{eff}, where the microwave field can serve as a rotation operator $U_i(\theta,\phi) = \exp(-i\frac{\sigma_z}{2}\phi_i)\exp(-i\frac{\sigma_y}{2}\theta_i)$, and the subscript i denotes the initial time quantities.

(2) *Adiabatic modulation of parameters.* We drive the adiabatic ramp $\theta(t) = v^2t^2/(2\pi)$ with different fixed ϕ in different runs of the experiment, and hence, $\Theta(t)$ becomes a Fresnel function generated by the arbitrary wave-form generator. This kind of ramp has been implemented in Ref. [48].

(3) *Final time quantum projective measurement.* In the final time t_f, the SAH or energy fluctuation operator of the effective Hamiltonian can be measured through fluorescence detection during optical excitation [44,48,49]. For example, in order to measure the energy fluctuation, we can get the population of the final effective Hamiltonian in repeated experiments, from which we can obtain the energy fluctuation. The final state after the adiabatic ramp is projected into either eigenstate of the final time effective Hamiltonian, which can be realized via a different rotation operator $U_f^\dagger(\theta,\phi) = \exp(i\frac{\sigma_y}{2}\theta_f)\exp(i\frac{\sigma_z}{2}\phi_f)$ from $U_i^\dagger(\theta,\phi)$ before the spin-selective fluorescence readout, and the subscript f denotes the final time quantities. In more complex scenarios, such as many-body situations, finding some observables commuting with the final time Hamiltonian is favorable to reconstruct the transition amplitude $p_{n|0}$, which denotes the probability of a state starting from the ground state of initial Hamiltonian and ending up in the nth eigenstate of the final Hamiltonian [50].

Compared with Refs. [9,47], we do not need to determine the resonant frequency during the process of parametric modulation, which is equal to the energy gap between the eigenstates of the effective Hamiltonian Eq. (24). Instead, we only set the adiabatic ramp velocity without prior measurement. Besides, the adiabatic ramp is not limited to periodically small perturbation. Due to the importance of the energy fluctuation in quantum physics, the measurement schemes concerning energy fluctuation are widely discussed [44,50–56], which provides our scheme with great potential.

The NV center has been the device for measuring the QFI using the method in Ref. [7]. The experimental results have been demonstrated in Refs. [9,47]. We utilize our measuring protocol to carry out the numerical simulation with the practical parameters given in Refs. [9,47]. The system we make use of is the NV electronic spin coupled by a ^{13}C nuclear spin, for which the interacting two-qubit effective Hamiltonian in a rotating frame the same as $e^{iR(t)}$ is given by Ref. [9]:

$$\begin{aligned} H_{\text{eff}}(\theta,\phi) \simeq{}& \frac{\Omega_{\text{mw}}}{2} \times [\cos\theta\sigma_z + \sin\theta(\cos\phi\sigma_x + \sin\phi\sigma_y)] \\ &+ \left(\frac{\gamma_n B_{||}}{2} - \frac{A_z}{4}\right)\tau_z - \frac{A_x}{4}\tau_x - \frac{A_z}{4}\sigma_z\otimes\tau_z \\ &- \frac{A_x}{4}\sigma_z\otimes\tau_x, \end{aligned} \tag{25}$$

where Ω_{mw} is the amplitude including an electron gyromagnetic ratio, and A_x and A_z are the hyperfine coupling parameters. γ_n is the nuclear spin gyromagnetic ratio, and $B_{||}$ is the external magnetic field. In Fig. 5 we give the QFIs F_θ and F_ϕ of the ground state of the Hamiltonian Eq. (25) for different values of θ when $\phi = 0$ is set. The simulation result coincides with that in Ref. [9] well.

IV. EXTENSIONS TO THE STATISTICAL MODELS

The QFI has been considered to be the key to studying quantum phase transitions. Since our method gives a direct measurement of the QFI, we will examine the result obtained from the adiabatic perturbation theory and discuss whether the signal of the quantum phase transition is still clear.

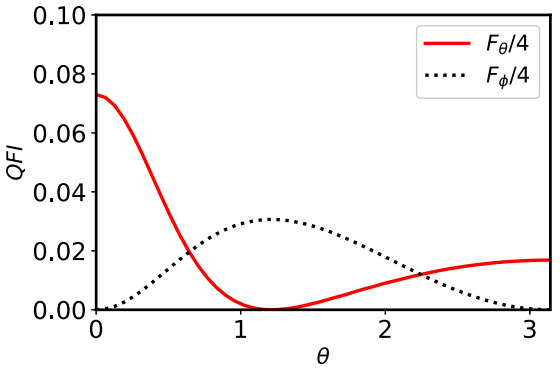

FIG. 5. QFI of θ and ϕ in a rotating frame interacting two-qubit model, which is experimentally measured in [9]. The result using our method with the same parameters is exactly coincident with that of [9]. We list the actual parameters here: $A_x = 2.79\,\mathrm{MHz}$, $A_z = 11.832\,\mathrm{MHz}$, $\Omega_{\mathrm{mw}} = 2.13\,\mathrm{MHz}$, $\gamma_n B_{||} = 1.07\times749.32\,\mathrm{kHz}$, and $\phi = 0$.

A. Transverse-field Ising model

The famous one-dimensional transverse-field Ising model is always the first model to detect new physics under the situation of phase transition. We study the following model [38],

$$H(t) = -J\sum_{i=1}^{N}\sigma_i^x\sigma_{i+1}^x - B(t)\sum_{i=1}^{N}\sigma_i^z, \tag{26}$$

where J is the coupling strength between neighboring spins, and $B(t)$ is the external magnetic field along the z direction. We fix the coupling strength $J = 10$ and modify the field $B(t) = 5 + \frac{v^2t^2}{4h}$ to obtain the QFI, where the field approaches the artificial value $(5 + h)$ at the final time $t_f = \frac{2h}{v}$. We can adjust the evolving speed v and the preset value h. Through changing the value h, we can measure the QFI of the ground state at arbitrary external magnetic field $B(t)$. The initial value of the magnetic field is set to be $B(0) = 5J$ to lift the possible degeneracy of energy levels.

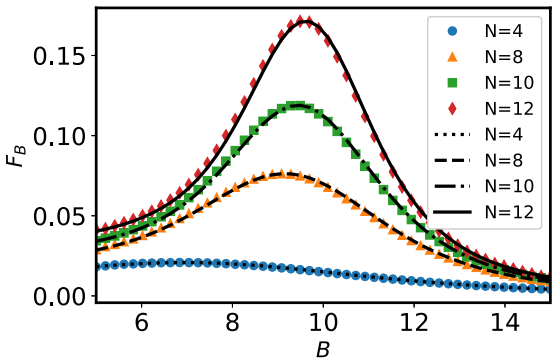

FIG. 6. QFI of the ground state of transverse-field Ising model with respect to the field strength. The dot is the measured quantum Fisher information using our method, while the line is the analytic solution using Eq. (28). In our case, the positive parity is used since the energy is lower in the situation of positive parity.

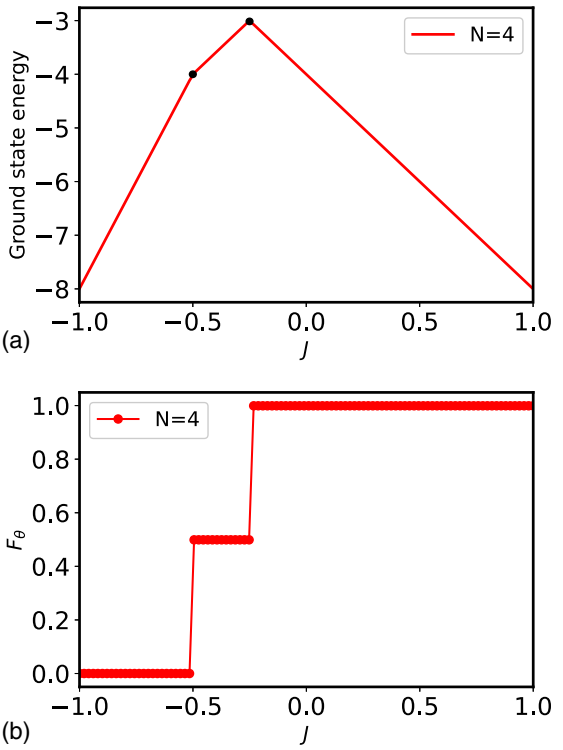

FIG. 7. (a) Level crossing of the ground state of the Heisenberg spin chain. In the considered region of the coupling strength, level crossing occurs twice at $J = -0.5$ and $J = -0.25$, respectively. (b) QFI with respect to the field strength of the ground state of the Heisenberg spin chain. We obtain the QFI using our method. It is apparent that the QFI also shows two abrupt changes at the corresponding values of J, which depicts the level crossing.

The ground state of the Hamiltonian is

$$|\phi_0\rangle = \prod_{k>0}(\cos\theta_k|0\rangle_k|0\rangle_{-k} + i\sin\theta_k|1\rangle_k|1\rangle_{-k}), \tag{27}$$

where $|0\rangle_k$ and $|1\rangle_k$ are the number states of the k-space fermionic operator before the Bogoliubov transformation. The quantum Fisher information with respect to the external field is evaluated to be [57–60]

$$F_B = \sum_{k>0}\frac{J^2\sin^2 k}{(J^2 + B^2 - 2JB\cos k)^2}. \tag{28}$$

The peak value of the QFI with respect to the external field should emerge at $B = 10$ when $J = 10$, corresponding to the phase transition point. Limited by the dimension of the Hilbert space, we give the QFI when the number of spins is $N = 4, 8, 10, 12$. We can see from the Fig. 6 that the peak value becomes gradually distinct when the magnetic field $B = 10$, which coincides with the theoretical conclusion of this model. It is obvious that the measured quantum Fisher information using our method matches the analytic solution Eq. (28) perfectly.

B. Heisenberg spin chain

Here we give another example of application of our measured quantum Fisher information. For the generalized

Heisenberg spin chain, when we focus on the coupling strength, the phase transition due to the energy level crossing emerges under this situation. The Heisenberg spin chain in an external magnetic field [14],

$$H = -J\sum_{i=1}^{N}\boldsymbol{\sigma}_i\cdot\boldsymbol{\sigma}_{i+1} - \sum_{i=1}^{N}\boldsymbol{h}(t)\cdot\boldsymbol{\sigma}_i, \tag{29}$$

reveals the contribution of level crossing, where $\boldsymbol{h}(t) = (\sin\theta(t), 0, \cos\theta(t))$ and $\theta = \frac{v^2t^2}{2\pi}$. The QFI corresponding to the ground state with respect to θ at the final time $t = \frac{\pi}{v}$ is obtained from our method, and we plot it as a function of the coupling strength J in Fig. 7(b).

The final Hamiltonian is actually isotropic spin interaction with an x-direction field. Figure 7(a) denotes the level crossing of the ground state of the final Hamiltonian, and Fig. 7(b) exhibits the step at the corresponding J. Without calculating the exact form of the ground state, we can obtain the fact that the QFI of the ground state with respect to the parameter θ only changes when the coupling strength J causes the level crossing. The extracted Berry curvature can exhibit such properties as in Ref. [14].

V. CONCLUSION AND DISCUSSION

In this article an alternate way is shown to derive the link between SAH or energy fluctuation and the QFI or QFIM. The adiabatic perturbation setup has been employed to measure the Berry curvature via the measurement of the generalized force both numerically and experimentally; hence the extraction of QFI or QFIM can also be applied to the same schemes except the final measured quantity. However, few discussions are carried out. This setup also enables the direct extraction of the quantum geometric tensor. All we need to do is change the estimating parameter relatively slowly with zero initial velocity, followed by the measurement of the SAH or energy fluctuation at the final interested moment.

We have adopted two-level systems to testify as to the measurement of QFI and QFIM, and both of the extracted values match the analytical results well. An NV center simulation is made using the practical parameters, and it fits the experimental results exactly. The actual energy gap is so large that the parameters' change can be fast enough to fulfill the procedure in the time of magnitude μs. As a result, the NV center can truly exhibit our scheme. Also, the phase transition and level crossing can also be depicted in this protocol like the Berry curvature.

Besides the NV center implementation, extension of this scheme to many-body cases is also promising. In fact, the many-body states are often difficult to reconstruct completely. Hence, the extraction of QFI of many-body states is important in the absence of states' full information. Our schemes exhibit potential for this purpose, since we only need the measurement of energy fluctuation rather than the states' full information. Also, it is worth noting that our schemes benefit from the discussions of Hamiltonian identification [61–63], since the Hamiltonian of systems should be determined prior to the measurement. In summary, we believe our discussions will facilitate the practical application of the adiabatic perturbation theory in the direct extraction of Berry curvature and QFI, or the full quantum geometric tensor.

ACKNOWLEDGMENTS

This work was supported by the National Natural Science Foundation of China (Grants No. 11935012, No. 12175075, and No. 61871162).

APPENDIX: ENERGY FLUCTUATION IN ORIGINAL AND ROTATING FRAME

We now compare the energy fluctuation in the original frame and that of the rotating frame. We denote the original frame Hamiltonian and evolving state $H(t)$ and $|\psi(t)\rangle$, respectively. Meanwhile, the rotating frame Hamiltonian and evolving state are $H_{\rm eff}(t)$ and $|\phi(t)\rangle$, respectively. Under the rotation of $e^{iR(t)}$, we then have

$$|\psi(t)\rangle = e^{-iR(t)}|\phi(t)\rangle \tag{A1}$$

and

$$H_{\rm eff} = e^{iR(t)}He^{-iR(t)} + i\frac{\partial e^{iR(t)}}{\partial t}e^{-iR(t)}. \tag{A2}$$

As a result, the energy fluctuation in the original frame reads

$$\langle\Delta^2 H(t)\rangle = \langle\psi(t)|H^2(t)|\psi(t)\rangle - \langle\psi(t)|H(t)|\psi(t)\rangle^2, \tag{A3}$$

while that of rotating frame becomes

$$\langle\Delta^2 H_{\rm eff}\rangle_r = \langle\phi(t)|H_{\rm eff}^2(t)|\phi(t)\rangle - \langle\phi(t)|H_{\rm eff}(t)|\phi(t)\rangle^2, \tag{A4}$$

where the subscript r represents the expectation in the rotating frame evolving state $|\phi(t)\rangle$.

When we substitute (A2) into (A4) and assume $[dR(t)/dt, R(t)] = 0$, we find

$$\langle\Delta^2 H_{\rm eff}\rangle_r = \langle\psi(t)|\left[\Delta^2 H(t) - 2{\rm Cov}\left(H, \frac{dR(t)}{dt}\right) + \Delta^2\left(\frac{dR(t)}{dt}\right)\right]|\psi(t)\rangle = \langle\Delta^2 H'\rangle, \tag{A5}$$

where $H' = H - dR(t)/dt$. In our case, $H' = V(t_f)\sigma_x$ at final time t_f, where $\cos\theta(t_f) = 0$. Hence, we measure σ_x in the original frame, which can also lead to the result of energy fluctuation in the rotating frame. The procedures in Sec. III involve a rotation prior to the final measurement, which works in wider situations such as $\theta(t_f) \neq 0$.

[1] C. L. Degen, F. Reinhard, and P. Cappellaro, Rev. Mod. Phys. **89**, 035002 (2017).
[2] J. Liu, H. Yuan, X.-M. Lu, and X. Wang, J. Phys. A: Math. Theor. **53**, 023001 (2020).
[3] X.-M. Lu, X. Wang, and C. P. Sun, Phys. Rev. A **82**, 042103 (2010).
[4] P. Hauke, M. Heyl, L. Tagliacozzo, and P. Zoller, Nat. Phys. **12**, 778 (2016).
[5] A. S. Holevo, *Probabilistic and Statistical Aspects of Quantum Theory*, Vol. 1 (Springer Science & Business Media, New York, 2011).
[6] C. W. Helstrom, J. Stat. Phys. **1**, 231 (1969).

[7] T. Ozawa and N. Goldman, Phys. Rev. B **97**, 201117(R) (2018).
[8] F. Fröwis, P. Sekatski, and W. Dür, Phys. Rev. Lett. **116**, 090801 (2016).
[9] M. Yu, P. Yang, M. Gong, Q. Cao, Q. Lu, H. Liu, S. Zhang, M. B. Plenio, F. Jelezko, T. Ozawa, N. Goldman, and J. Cai, Natl. Sci. Rev. **7**, 254 (2020).
[10] X. Tan, D.-W. Zhang, Z. Yang, J. Chu, Y.-Q. Zhu, D. Li, X. Yang, S. Song, Z. Han, Z. Li, Y. Dong, H.-F. Yu, H. Yan, S.-L. Zhu, and Y. Yu, Phys. Rev. Lett. **122**, 210401 (2019).
[11] A. Rath, C. Branciard, A. Minguzzi, and B. Vermersch, Phys. Rev. Lett. **127**, 260501 (2021).
[12] M. Yu, D. Li, J. Wang, Y. Chu, P. Yang, M. Gong, N. Goldman, and J. Cai, Phys. Rev. Res. **3**, 043122 (2021).
[13] H.-T. Ding, Y.-Q. Zhu, P. He, Y.-G. Liu, J.-T. Wang, D.-W. Zhang, and S.-L. Zhu, Phys. Rev. A **105**, 012210 (2022).
[14] V. Gritsev and A. Polkovnikov, Proc. Natl. Acad. Sci. USA **109**, 6457 (2012).
[15] Y.-Q. Ma, S. Chen, H. Fan, and W.-M. Liu, Phys. Rev. B **81**, 245129 (2010).
[16] O. Bleu, G. Malpuech, Y. Gao, and D. D. Solnyshkov, Phys. Rev. Lett. **121**, 020401 (2018).
[17] J. Provost and G. Vallee, Commun. Math. Phys. **76**, 289 (1980).
[18] A. Gianfrate, O. Bleu, L. Dominici, V. Ardizzone, M. De Giorgi, D. Ballarini, G. Lerario, K. West, L. Pfeiffer, D. Solnyshkov *et al.*, Nature (London) **578**, 381 (2020).
[19] D. Xiao, M.-C. Chang, and Q. Niu, Rev. Mod. Phys. **82**, 1959 (2010).
[20] S. Sugawa, F. Salces-Carcoba, A. R. Perry, Y. Yue, and I. B. Spielman, Science **360**, 1429 (2018).
[21] M. Kolodrubetz, Phys. Rev. Lett. **117**, 015301 (2016).
[22] M. Kolodrubetz, Phys. Rev. B **89**, 045107 (2014).
[23] T. T. Luu and H. J. Wörner, Nat. Commun. **9**, 916 (2018).
[24] N. Fläschner, B. S. Rem, M. Tarnowski, D. Vogel, D.-S. Lühmann, K. Sengstock, and C. Weitenberg, Science **352**, 1091 (2016).
[25] J. Avron, M. Fraas, and G. Graf, J. Stat. Phys. **148**, 800 (2012).
[26] J. E. Avron, M. Fraas, G. M. Graf, and O. Kenneth, New J. Phys. **13**, 053042 (2011).
[27] C. De Grandi and A. Polkovnikov, in *Quantum Quenching, Annealing and Computation*, edited by A. K. Chandra, A. Das, and B. K. Chakrabarti (Springer, Berlin, Heidelberg, 2010), pp. 75–114.
[28] G. Rigolin, G. Ortiz, and V. H. Ponce, Phys. Rev. A **78**, 052508 (2008).
[29] G. Rigolin and G. Ortiz, Phys. Rev. A **90**, 022104 (2014).
[30] G. Rigolin and G. Ortiz, Phys. Rev. Lett. **104**, 170406 (2010).
[31] M. Kolodrubetz, D. Sels, P. Mehta, and A. Polkovnikov, Phys. Rep. **697**, 1 (2017).
[32] C. D. Grandi, A. Polkovnikov, and A. W. Sandvik, J. Phys.: Condens. Matter **25**, 404216 (2013).
[33] M. D. Schroer, M. H. Kolodrubetz, W. F. Kindel, M. Sandberg, J. Gao, M. R. Vissers, D. P. Pappas, A. Polkovnikov, and K. W. Lehnert, Phys. Rev. Lett. **113**, 050402 (2014).
[34] P. Xu, A. H. Kiilerich, R. Blattmann, Y. Yu, S.-L. Zhu, and K. Mølmer, Phys. Rev. A **96**, 010101(R) (2017).
[35] P. Xu, S.-L. Zhu, K. Mølmer, and A. H. Kiilerich, Phys. Rev. A **102**, 032613 (2020).
[36] Q.-X. Lv, Y.-X. Du, Z.-T. Liang, H.-Z. Liu, J.-H. Liang, L.-Q. Chen, L.-M. Zhou, S.-C. Zhang, D.-W. Zhang, B.-Q. Ai, H. Yan, and S.-L. Zhu, Phys. Rev. Lett. **127**, 136802 (2021).
[37] M. Kolodrubetz, V. Gritsev, and A. Polkovnikov, Phys. Rev. B **88**, 064304 (2013).
[38] S.-J. Gu, Int. J. Mod. Phys. B **24**, 4371 (2010).
[39] M. V. Berry and J. Robbins, Proc. R. Soc. London A **442**, 659 (1993).
[40] J. Johansson, P. Nation, and F. Nori, Comput. Phys. Commun. **183**, 1760 (2012).
[41] M. Zhang, H.-M. Yu, H. Yuan, X. Wang, R. Demkowicz-Dobrzański, and J. Liu, Phys. Rev. Res. **4**, 043057 (2022).
[42] M. W. Doherty, N. B. Manson, P. Delaney, F. Jelezko, J. Wrachtrup, and L. C. Hollenberg, Phys. Rep. **528**, 1 (2013).
[43] M. W. Doherty, F. Dolde, H. Fedder, F. Jelezko, J. Wrachtrup, N. B. Manson, and L. C. L. Hollenberg, Phys. Rev. B **85**, 205203 (2012).
[44] S. Hernández-Gómez, N. Staudenmaier, M. Campisi, and N. Fabbri, New J. Phys. **23**, 065004 (2021).
[45] V. Dobrovitski, G. Fuchs, A. Falk, C. Santori, and D. Awschalom, Annu. Rev. Condens. Matter Phys. **4**, 23 (2013).
[46] Y.-N. Lu, Y.-R. Zhang, G.-Q. Liu, F. Nori, H. Fan, and X.-Y. Pan, Phys. Rev. Lett. **124**, 210502 (2020).
[47] M. Yu, Y. Liu, P. Yang, M. Gong, Q. Cao, S. Zhang, H. Liu, M. Heyl, T. Ozawa, N. Goldman *et al.*, npj Quantum Inf. **8**, 56 (2022).
[48] W. Ma, L. Zhou, Q. Zhang, M. Li, C. Cheng, J. Geng, X. Rong, F. Shi, J. Gong, and J. Du, Phys. Rev. Lett. **120**, 120501 (2018).
[49] S. Hernández-Gómez, S. Gherardini, F. Poggiali, F. S. Cataliotti, A. Trombettoni, P. Cappellaro, and N. Fabbri, Phys. Rev. Res. **2**, 023327 (2020).
[50] M. Herrera, J. P. S. Peterson, R. M. Serra, and I. D'Amico, Phys. Rev. Lett. **127**, 030602 (2021).
[51] S. Gherardini, A. Belenchia, M. Paternostro, and A. Trombettoni, Phys. Rev. A **104**, L050203 (2021).
[52] A. J. Roncaglia, F. Cerisola, and J. P. Paz, Phys. Rev. Lett. **113**, 250601 (2014).
[53] G. Watanabe, B. P. Venkatesh, and P. Talkner, Phys. Rev. E **89**, 052116 (2014).
[54] M. Campisi, P. Hänggi, and P. Talkner, Rev. Mod. Phys. **83**, 771 (2011).
[55] M. Esposito, U. Harbola, and S. Mukamel, Rev. Mod. Phys. **81**, 1665 (2009).
[56] D. Yang, A. Grankin, L. M. Sieberer, D. V. Vasilyev, and P. Zoller, Nat. Commun. **11**, 775 (2020).
[57] P. Zanardi, P. Giorda, and M. Cozzini, Phys. Rev. Lett. **99**, 100603 (2007).
[58] L. Campos Venuti and P. Zanardi, Phys. Rev. Lett. **99**, 095701 (2007).
[59] P. Zanardi and N. Paunković, Phys. Rev. E **74**, 031123 (2006).
[60] H. T. Quan, Z. Song, X. F. Liu, P. Zanardi, and C. P. Sun, Phys. Rev. Lett. **96**, 140604 (2006).
[61] D. Burgarth and K. Maruyama, New J. Phys. **11**, 103019 (2009).
[62] J. Zhang and M. Sarovar, Phys. Rev. Lett. **113**, 080401 (2014).
[63] S. G. Schirmer, A. Kolli, and D. K. L. Oi, Phys. Rev. A **69**, 050306(R) (2004).